Control of series multicell converters by linear state feedback decoupling

Olivier Tachon, Maurice Fadel, Thierry Meynard

▶ **To cite this version:**

Olivier Tachon, Maurice Fadel, Thierry Meynard. Control of series multicell converters by linear state feedback decoupling. 7th European Conference on Power Electronics and Applications EPE' 97, Sep 1997, Trondheim, Norway. pp.588-593. hal-03554190

HAL Id: hal-03554190
https://hal.science/hal-03554190

Submitted on 3 Feb 2022

HAL is a multi-disciplinary open access archive for the deposit and dissemination of scientific research documents, whether they are published or not. The documents may come from teaching and research institutions in France or abroad, or from public or private research centers.

L'archive ouverte pluridisciplinaire **HAL**, est destinée au dépôt et à la diffusion de documents scientifiques de niveau recherche, publiés ou non, émanant des établissements d'enseignement et de recherche français ou étrangers, des laboratoires publics ou privés.

CONTROL OF SERIES MULTICELL CONVERTERS BY LINEAR STATE FEEDBACK DECOUPLING

O. Tachon, M. Fadel, T. Meynard

Laboratoire d'Electrotechnique et d'Electronique Industrielle, Toulouse France

Abstract: The paper presents the study of control laws applied to series multicell converters. This multi-variable system requires control laws based on linear state feedback decoupling to ensure a selective interaction between inputs and outputs and assign the dynamics of state-variables.

Keywords: high voltage, multicell converters, modelling, control, state feedback, decoupling

INTRODUCTION

In the field of high voltage power conversion, a new multilevel topology has been introduced in the early 1990's: the multicell converters [1] [2]. These converters enable reaching high power/ high voltage applications with standard semiconductors.

A specific feature of this structure is the flying voltage sources, realized by capacitors, which solve the problem of static and dynamic sharing of the voltage across the blocking switches.

The presence of the flying capacitors and the independent control of each commutation cell make this converter a multi-variable and non-linear system which is characterized by an interaction between the capacitors voltage and the load current.

In order to solve the coupling problem, a method based on linear state feedback decoupling is developed. This method applied in static converter control is derived of the decoupling principle which has been implemented in induction motor drives [3] [4] in the non-linear cases.

In this paper, after having introduced the converter model, the decoupling principle is reviewed and applied to a three-cell chopper operating in the buck mode. We show that the input-output decoupling allows to minimize the interaction among the state-variables and provide fast transients.

MODELLING MULTICELL CONVERTERS

The structure of multicell converters operating in the step-down mode is represented in figure 1. It is composed of p commutation cells connected with (p-1) flying capacitors.

The flying capacitors voltage should be equal to: $v_{C_k} = k \cdot E/p$ $(k = 1 \cdots p-1)$ so that the voltage applied across the k^{th} cell is constant and equal to: $v_{Cel_k} = v_{C_k} - v_{C_{k-1}} = E/p$.

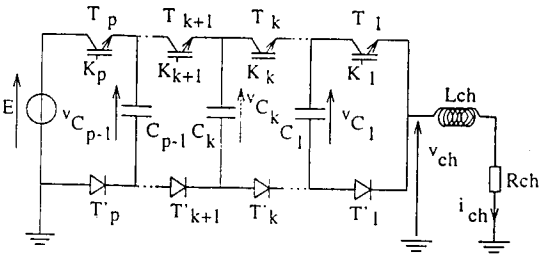

FIG. 1 – *Multicell buck chopper*

It has been shown [5] that this voltage balance is obtained when the duty cycles of the different commutation cells are equal and the phase-shift is $2\,\pi/p$.
In this case, the output wave v_{ch} is modulated between two levels distant by E/p with a frequency which is p times the switching frequency.

In the structure (figure 1), each capacitor C_k is connected between switches T_k and T_{k+1} controlled by the control signals K_k and K_{k+1}. The variables K_k and K_{k+1} represent the switch state 0 or 1 and will be used as inputs for the modelling.

The modelling of static converters for control design purpose is difficult because these systems involve continuous elements (inductors, capacitors) as well as discrete elements (switches) and the operation of converter is a periodic sequence of different stages.
Two models of the multicell converter have been derived [6]:

- the instantaneous model which takes the switching behaviour into account,
- the averaged model in which the varying quantities are assimilated to their average value over a switching period.

Before introducing the models, we formulate the following assumptions:

- the switches are ideal (on-state voltage, off-state current, dead times, delays and switching times are null),
- the flying capacitors are designed to limit the variation of voltage applied to each commutation cell.

Instantaneous model

The evolution of the state variables (flying voltage v_{C_k} and load current i_{ch} for a multicell buck chopper) is given by the following equations:

$$\frac{d}{dt}v_{C_k} = \frac{i_{ch}}{C_k}[K_{k+1} - K_k] \quad (1)$$

$$\frac{d}{dt}i_{ch} = -\frac{R_{ch}}{L_{ch}}i_{ch} + \frac{E}{L_{ch}}K_p + \frac{v_{C_{p-1}}}{L_{ch}}[K_{p-1} - K_p] + \cdots + \frac{v_{C_k}}{L_{ch}}[K_k - K_{k+1}] + \cdots + \frac{v_{C_1}}{L_{ch}}[K_1 - K_2] \quad (2)$$

These equations exhibit the non-linear character of the model and form a non linear state system: $\dot{x} = A \cdot x + B(x) \cdot u$. The state vector x is composed of $v_{C_1}, \cdots, v_{C_{p-1}}, i_{ch}$ and the control signals $K_1, \cdots, K_p$ make the command vector u.

The instantaneous model will be used to validate the control laws developed with the average model which is introduced below.

Average model

In this model, each quantity is replaced with its average value over a switching period.
Hence, the control signals are now the duty cycles $\mathcal{R}_k$ of the commutation cells which are the average values of the variables K_k.

The circulating current in flying capacitor C_k is defined by the state of two adjacent cells:

$$I_{C_k} = [\mathcal{R}_{k+1} - \mathcal{R}_k]\, I_{ch} \quad (3)$$

where I_{ch} is the average load current.

We define new variables α_k which are the difference between the duty cycles $\mathcal{R}_{k+1}$ and $\mathcal{R}_k$, and form a new control vector. Thus the flying voltage v_{C_k} will be controlled by α_k . The average model is described by the non linear dynamic state equation:

$$\dot{x} = A_1 \cdot x + B_1(x) \cdot u \quad (4)$$

where

$$A_1 = \begin{pmatrix} 0 & \cdots & 0 & 0 \\ \vdots & \ddots & \vdots & \vdots \\ 0 & \cdots & 0 & 0 \\ 0 & \cdots & 0 & -\frac{R_{ch}}{L_{ch}} \end{pmatrix}$$

$$B_1 = \begin{pmatrix} \frac{I_{ch}}{C_1} & 0 & \cdots & 0 & 0 \\ 0 & \ddots & \ddots & \vdots & \vdots \\ \vdots & \ddots & \frac{I_{ch}}{C_{p-2}} & 0 & 0 \\ 0 & \cdots & 0 & \frac{I_{ch}}{C_{p-1}} & 0 \\ -\frac{Vc_1}{L_{ch}} & \cdots & -\frac{Vc_{p-2}}{L_{ch}} & -\frac{Vc_{p-1}}{L_{ch}} & \frac{E}{L_{ch}} \end{pmatrix}$$

$$x = [V_{C_1} \cdots V_{C_k} \cdots V_{C_{p-1}}\ I_{ch}],$$
$$u = [\alpha_1 \cdots \alpha_k \cdots \alpha_{p-1}\ \mathcal{R}_p], \quad (5)$$

The dimensions of the matrix A_1 and B_1 are $p \times p$ (p is the number of state variables/ and number of commutation cells).

In order to apply the multi-variable theory, the non-linear average model has been linearized around an operating point by the local linear method.
The linearized system is defined by equation 6:

$$\delta\dot{x} = A_2 \cdot \delta x + B_2(x_0) \cdot \delta u \quad (6)$$

where $\delta x = [\delta V_{C_1} \cdots \delta V_{C_{p-1}}\ \delta I_{ch}]$ is the linearized state vector, $\delta u = [\delta\alpha_1 \cdots \delta\alpha_{p-1}\ \delta\mathcal{R}_p]$ the linearized control vector and x_0 represents the operating point which is defined by $[V_{C_{1_0}} \cdots V_{C_{p-1_0}} E_0\ I_{ch_0}]$.

Matrix A_2 is identical with matrix A_1 and matrix B_2 is obtained from B_1 by putting the variables $V_{C_{1_0}}, \cdots, V_{C_{p-1_0}}, E_0,\ I_{ch_0}$ in place of variables $V_{C_1}, \cdots, V_{C_{p-1}}, E,\ I_{ch}$.

LINEAR STATE FEEDBACK DECOUPLING

In multidimensional process, any input can influence any output.

The objective of the input-output decoupling is to find a state feedback such that each input influences only one output. This allows modelling the system as a set of mono-variable subsystems evolving in parallel.

Moreover, to solve the coupling phenomena, the number of inputs must be higher than or equal to the number of outputs.

Decoupling procedure

The decoupling procedure is described in [7] and defines the matrices R and L which compose the state feedback:

$$u = -R \cdot x + L \cdot e \quad (7)$$

where e represents the new input vector.

For a linear system S ($\dot{\delta x} = A \cdot \delta x + B \cdot \delta u$ and $y = C \cdot \delta x$), a sufficient and necessary condition to compute matrices R and L is that matrix $\mathcal{J}$ defined below must be inversible:

$$\mathcal{J} = \begin{pmatrix} {}_1CA^{d_1}B \\ \vdots \\ {}_nCA^{d_n}B \end{pmatrix} \quad (8)$$

where n is the dimension of the state vector, ${}_kC$ represents the k^{th} line of matrix C and the index d_k is defined as the smallest power of matrix A which gives ${}_kCA^{d_k}B \neq 0$.
Obtaining index d_k allows to calculate the matrix A^* defined by:

$$A^* = \begin{pmatrix} {}_1CA^{d_1+1} \\ \vdots \\ {}_nCA^{d_n+1} \end{pmatrix} \quad (9)$$

These two matrices $\mathcal{J}$ and A^* permit to determine an intermediate system $\overline{S}$: $\dot{x} = [A - B \cdot \mathcal{J}^{-1} \cdot A^*] \cdot x + B \cdot \mathcal{J}^{-1} \cdot u$ corresponding to integral decoupled system where each output k is the $(d_k + 1)^{th}$ integral of the input k.
Afterwards, we apply a state compensation to this system $\overline{S} : u = -\overline{R} \cdot x + \overline{L} \cdot e$ with:

$$\overline{R} = \begin{pmatrix} p_1 & & 0 \\ & \ddots & \\ 0 & & p_n \end{pmatrix} \quad \overline{L} = -\overline{R} \qquad (10)$$

Variables p_k represent assigned dynamics on state variables ($p_k < 0$, $k = 1 \cdots n$) and $\overline{L}$ is chosen equal to $-\overline{R}$ in order to obtain a unit gain in close-loop.

Matrices R and L which ensure the decoupling are derived from the previous matrices by the following relations:

$$R = \mathcal{J}^{-1} \cdot [\overline{R} - A^*] \qquad (11)$$
$$L = \mathcal{J}^{-1} \cdot \overline{L} \qquad (12)$$

The control structure is represented in figure 2

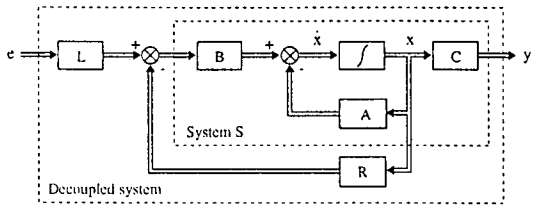

FIG. 2 – *Structure of the state feedback decoupling*

The method is a classical state feedback but it is the particular calculation of matrices R et L which guarantees a selective interaction between the inputs/outputs and assigns the dynamics of state variables.

Application to multicell converters

The theorical development is executed with the linear state system described in equation 6. The verification of the sufficient condition uses the matrix C which is not defined in system 6. In our case, this one is the identity matrix of dimension n.

Figure 3 represents the linear state feedback decoupling applied to a multicell buck chopper.

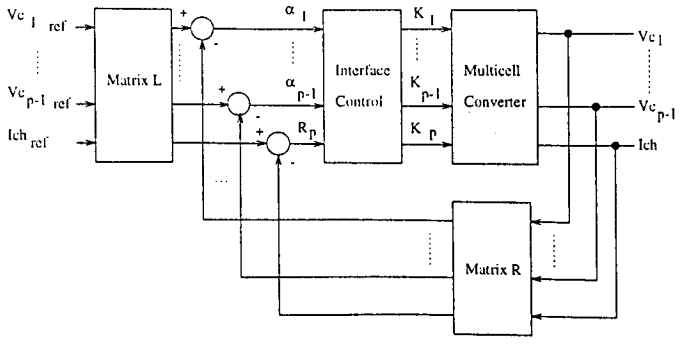

FIG. 3 – *State feedback decoupling applied to multicell converter*

The input vector is composed of reference values $v_{C_{1_{ref}}}, \cdots, v_{C_{p-1_{ref}}}$, $i_{ch_{ref}}$ of each controlled variables $v_{C_1} \cdots v_{C_{p-1}}$ i_{ch}. In the frequency domain, the state feedback decoupling implies that the transfer matrix in closed-loop is diagonal and is composed of first order transfer function.

The analytical form of matrices R and L is given by equation 13 in 3-cell buck chopper in order to simplify the expressions:

$$R = \begin{pmatrix} -\frac{C_1\ p_1}{I_{ch_0}} & 0 & 0 \\ 0 & -\frac{C_2\ p_2}{I_{ch_0}} & 0 \\ -\frac{C_1\ p_1\ V_{C_{1_0}}}{E_0\ I_{ch_0}} & -\frac{C_2\ p_2\ V_{C_{2_0}}}{E_0\ I_{ch_0}} & -\frac{L_{ch}\ p_3 + R_{ch}}{E_0} \end{pmatrix}$$

$$L = \begin{pmatrix} -\frac{C_1\ p_1}{I_{ch_0}} & 0 & 0 \\ 0 & -\frac{C_2\ p_2}{I_{ch_0}} & 0 \\ -\frac{C_1\ p_1\ V_{C_{1_0}}}{E_0\ I_{ch_0}} & -\frac{C_2\ p_2\ V_{C_{2_0}}}{E_0\ I_{ch_0}} & -\frac{L_{ch}\ p_3}{E_0} \end{pmatrix} \qquad (13)$$

The parameters of the control law extended to p-cell buck chopper are

- converter characteristics: $C_1, \cdots, C_{p-1}$,
- load characteristics: R_{ch}, L_{ch},
- operating point of linearization: $V_{C_{1_0}}, \cdots, V_{C_{p-1_0}}, E_0, I_{ch_0}$
- assigned dynamics $p_1, \cdots, p_{p-1}, p_p$.

Variable p_k sets the dynamic of flying capacitor voltage v_{C_k} ($k = 1, \cdots, p-1$) and variable p_p, the dynamic of load current i_{ch}. The corresponding time constants called τ_k are defined by $-1/p_k$

As matrices R and L have common terms which are $-\frac{C_k\ p_k}{I_{ch_0}}$ and $-\frac{C_k\ p_k\ V_{C_{1_0}}}{E_0\ I_{ch_0}}$, a transformation can be executed to simplify the control structure [8].

Figure 4 exhibits the simplified structure control for 3-cell buck chopper ($p = 3$).

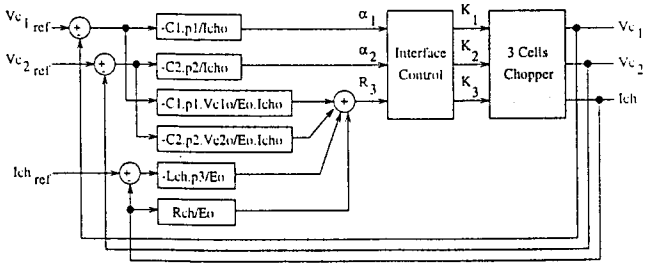

FIG. 4 – *Simplified control scheme of 3-cell chopper*

Choice of linearization point

Parameters $V_{C_{k_0}}$

The aim of the control is to regulate capacitor voltages v_{C_k} around the reference $v_{C_{k_{ref}}}$ equal to $v_{C_k} = k \cdot E/p$

to ensure equal voltage sharing among switches in off state.
Thus, parameters $v_{C_{k_0}}$ are chosen equal to $k \cdot E/p$ and are only used in the current regulation loop in a proportional manner.

The start-up with zero initial conditions exhibits a current overshoot. This is due to initial operating point (where $v_{C_1} \cdots v_{C_{p-1}}$ are null) which is very different from operating point of linearization $V_{C_{1_0}}, \cdots, V_{C_{p-1_0}}$.

Parameter I_{ch_0}

The choice of I_{ch_0} is a different matter because the multicell buck chopper is designed to operate in an entire current interval $[0; E/R_{ch}]$ as a conventionnel buck chopper.

This term I_{ch_0} influences the gains of the loops that control the capacitor voltages and the load current. The gains must be inversely proportional with I_{ch_0} so that I_{ch_0} cannot be equal to 0.

If the term I_{ch_0} is chosen equal to the steady state load current, dynamics of capacitor voltages v_{C_k} correspond to assigned dynamics p_k.
When the steady state current $i_{ch_{ref}}$ is different from I_{ch_0}, the dynamic of capacitor voltages p_k is modified and the time constant τ_k is multiplied by $I_{ch_0}/i_{ch_{ref}}$.

Moreover, a value of I_{ch_0} close to maximal load current (E/R_{ch}) allows minimizing the influence of terms $-\dfrac{C_k\, p_k\, V_{C_{1_0}}}{E_0\, I_{ch_0}}$ in current regulation loop.

Choice of dynamics

The dynamics p_k expressed in rad/s must be chosen in order to keep all modulation signals $\mathcal{R}_k$ ($\mathcal{R}_k = \mathcal{R}_{k+1} - \alpha_k$) included within interval [0;1]. The calculation of maximal dynamic implies to take the amplitudes of variations on state variables into account.

With this control structure, it is possible to give priority to the load current dynamic p_p or to the capacitor voltage dynamics p_k, depending on the application.

Nevertheless, the capacitor voltages dynamics will be identical to ensure voltage sharing across the switches even in transient state.

Robustness

In this part, we study the influences of the variations of the voltage supply E and of the load parameters R_{ch}, L_{ch} on the behaviour of control law where control parameters are kept constant. The variable p_p represents the assigned dynamic on the load current.

Supply voltage variation

The first consequence of the variations of the supply voltage E is a modification of the voltage references $(v_{C_{k_{ref}}} = k \cdot E/p)$.
However, the variations of the suplly voltage also induce variations of the coefficients in B_1 (equation 4) so that the closed-loop tranfer matrix of circuit in figure 2 is changed and the system is not fully decoupled. Moreover, the transfer function $i_{ch}/i_{ch_{ref}}$ becomes:

$$\frac{i_{ch}}{i_{ch_{ref}}} = \frac{E_1\, p_p}{E_0\, p'_p} \cdot \frac{1}{1 + \dfrac{s}{p'_p}} \qquad (14)$$

where E_1 is the new value of the voltage supply and p'_p represents the new dynamic defined by:

$$p'_p = \frac{E_1\, p_p}{E_0} + \frac{R_{ch}}{L_{ch}} \left[\frac{E_1 - E_0}{E_0}\right]. \qquad (15)$$

These equations (14 and 15) show that the steady-state gain and the dynamic of the load current i_{ch} are modified.

Load variations

Alike the voltage supply variation, a load variation involves a perturbation only on load current. The dynamic and steady-state gain are changing and the expression of the new transfer function is:

$$\frac{i_{ch}}{i_{ch_{ref}}} = \frac{1}{1 - \dfrac{\Delta_{Rch}}{L_{ch} \cdot p_3}} \cdot \frac{1}{1 + \dfrac{s}{p''_p}} \qquad (16)$$

where $\Delta_{Rch} = R_{ch_1} - R_{ch}$ (R_{ch_1} is the new resistor value) and p''_p represents the new dynamic defined by

$$p''_p = \frac{\Delta_{Rch} - L_{ch}\, p_3}{L_{ch}}. \qquad (17)$$

A load inductor variation implies a perturbation on load current dynamic and the new transfer function is:

$$\frac{i_{ch}}{i_{ch_{ref}}} = \frac{1}{1 - \dfrac{L_{ch_1}}{L_{ch}\, p_p}\, s} \qquad (18)$$

where L_{ch_1} represents the new inductor value.

Without perturbation, the state feedback assigns a first order transfer function between i_{ch} and $i_{ch_{ref}}$.
In order to minimize the disturbances due to fluctuations of load parameters and voltage supply, we place a PI controller in cascade with the state feedback on the load current loop (figure 5).

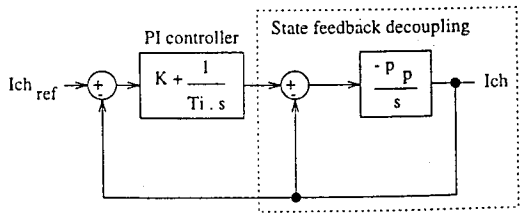

FIG. 5 – *Implementation of PI controller*

The controller parameters are chosen to keep a first order transfer function between i_{ch} and $i_{ch_{ref}}$: $K = 1$ and $\tau_i = -1/p_p$.
The PI controllers can be placed in capacitor voltages regulation loops in order to minimize the influence of switching times, dead times and any other perturbation of the duty cycles [9].

EXPERIMENTAL RESULTS

The performances of these control laws have been checked on a power test bench developed at the laboratory.

This power bench is based on 3-cell IGBT leg operating as a step-down chopper which has the following characteristics:

- maximum supply voltage: E=1800V,
- capacitors: $C_1 = 42\mu F$, $C_2 = 40\mu F$
- IGBT: Siemens 1200V 200A,
- switching frequency: f=16kHz,
- load resistor: 12Ω,
- load inductor: 1mH.

The regulation structure is implemented with a processor board dSPACE DS1102 which allows to control in real-time the operation of converter.

The preliminary results presented in this paper are obtained with a supply voltage E equal to 300V and the following parameters are identical for all tests: $V_{C_{1_0}} = 100V$ $V_{C_{2_0}} = 200V$ $E_0 = 300V$ $I_{ch_0} = i_{ch_{ref}}$.

Figure 6 shows the transient response for step changes in load current from 25A to 5A with an assigned dynamic p_3 of the load current equal to $-10000rad/s$. The dynamics of the capacitor voltages are defined by $p_1 = p_2 = -1000rad/s$.

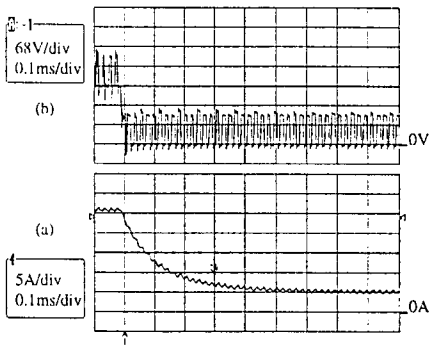

(a) load current $i_{ch}(A)$
(b) load voltage $v_{ch}(V)$

FIG. 6 – *Step of the current reference*

The load voltage waveform is modified to regulate the current; however this voltage waveform also shows that the cell voltages $(v_{C_k} - v_{C_{k-1}})$ stay balanced because the different voltage pulses have the same amplitude. As will be shown later (figure 8), a cell voltage unbalance can be detected from the load voltage waveform.

To illustrate the decoupling principle (figure 7), a variation on capacitor voltage v_{C_1} is applied such as $v_{C_{1_{ref}}} = v_{C_{2_{ref}}}$. The capacitor voltages dynamics are $p_1 = p_2 = -2000rad/s$ and the load current dynamic p_3 is equal to $-5000rad/s$.

Figure 8 shows an important unbalance of the load voltage v_{ch} due to the variation of $v_{C_{1_{ref}}}$. This unbalance implies a perturbation on the load current. The DC value is modified, but the increased harmonics are the main modification.

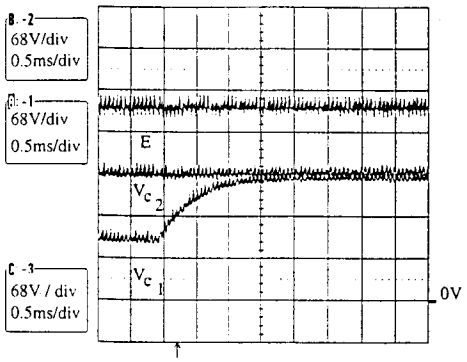

FIG. 7 – *Step of the reference voltage $v_{C_{1_{ref}}}$*

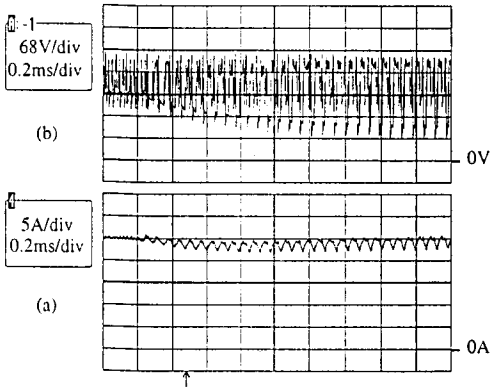

(a) load current $i_{ch}(A)$
(b) load voltage $v_{ch}(V)$

FIG. 8 – *Load waveforms in balanced and unbalanced mode*

The state feedback decoupling allows setting the dynamics on state variables. This is shown in figure 9 in a start-up where we assign two different dynamics. The reference load current is equal to 20A and the load current dynamic p_3 is equal to $-5000rad/s$.

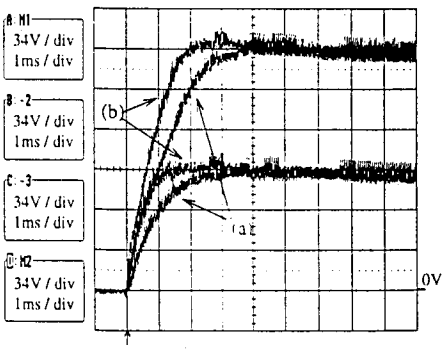

(a) dynamics $p_1 = p_2 = -1000rad/s$
(b) dynamics $p_1 = p_2 = -2000rad/s$

FIG. 9 – *Control of the flying capacitor voltages: influence of dynamics p_1 and p_2*

The dynamic of capacitor voltage v_{C_k} is function of $I_{ch_0}/i_{ch_{ref}}$. Figure 10 represents the voltage evolution across the flying capacitors in the cases $i_{ch_{ref}} = I_{ch_0} = 20A$ and $i_{ch_{ref}} = I_{ch_0}/2 = 10A$.

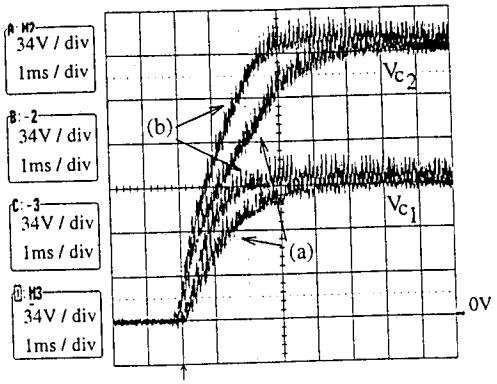

(a) $i_{ch_{ref}} = 20A$; $I_{ch_0} = 20A$
(b) $i_{ch_{ref}} = 10A$; $I_{ch_0} = 20A$

FIG. 10 – *Control of the flying capacitor voltages: influence of linearization point*

In the case a, the dynamic is equal to the assigned dynamic $p_1 = p_2 = -1000rad/s$. In the case b, the obtained dynamic is equal to the assigned dynamic divided by 2. Finally, we show the behaviour of PI controller in cascade with the state feedback decoupling for a load resistor variation from 12Ω to 8Ω (−33%). The reference current $i_{ch_{ref}}$ is equal to 15A as well as I_{ch_0}, and the time constant of integral term is defined $-1/p_3$.

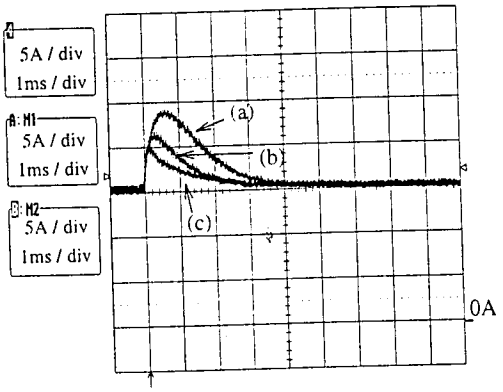

(a) dynamic $p_3 = -5000rad/s$
(b) dynamic $p_3 = -7000rad/s$
(c) dynamic $p_3 = -10000rad/s$

FIG. 11 – *Behaviour of PI controller*

The PI controller minimizes the effects of load variation more or less quickly according to its time constant.

CONCLUSION

The decoupling principle can be applied to the control of the multicell converters because the number of control signals are equal to the number of state variables.

Moreover, the state feedback decoupling allows to ensure load current variations without perturbations on the capacitor voltages and to assign the dynamics of the capacitor voltages.
Thus, the voltage sharing across the switches is preserved even in transient state.

The control law is calculated for a given operating point and its behaviour is quite disturbed when the converter does not operate at this point.
The choice of I_{ch_0} is important because if it is equal to a maximum load current , the dynamics of capacitor voltages will always be less than or equal to the assigned dynamics and there will be no saturation on the control signals.

The power test bench developed in the laboratory has allowed to validate the control laws at low voltage supply. The same equipment will then be tested at higher voltage levels.

REFERENCES

[1] T. Meynard and H. Foch, *Dispositif électronique de conversion d'énergie électrique*, 1991 French Patent n°91.09582 1992 International Patent P.C.T. n°92.00652 Europe, U.S.A., Japan, Canada.

[2] T. Meynard and H. Foch, "Multi-level conversion: high voltage choppers and voltage-source inverters," in *PESC*. Tolede, 1992, pp. 397–405.

[3] E. Ho and P. Sen, "Decoupling control of induction motor drives," *IEEE Transactions on Industrial Electronics*, vol. 35, no. 2, pp. 253–262, May 1988.

[4] A. Frick, E. von Westerholt, and B. de Fornel, "Non-linear control of induction motors via input-output decoupling," *ETEP*, vol. 4, no. 2, pp. 261–268, July-August 1994.

[5] T. Meynard, M. Fadel, and N. Aouda, "Modelling of multilevel converters," *IEEE Transactions on Industrial Electronics*, June 1997.

[6] O. Tachon, "Modélisation en vue de la simulation des convertisseurs multicellulaires série," in *FIRELEC*. JCGE, Avril 1996, pp. 82–86.

[7] E.G. Gilbert, "The decoupling of multivariable systems by state feedback," *S.I.A.M Journal of Control*, vol. 7, no. 1, pp. 50–63, Feb 1969.

[8] O. Tachon, M. Fadel, T. Meynard, and P. Carrere, *Dispositif électronique de conversion d'énergie électrique*, 1996 French Patent n°96.16192.

[9] O. Tachon, M. Fadel, T. Meynard, and L. Yacoubi, "Convertisseurs multicellulaires série: influence des imperfections des signaux de commande," in *EPF'96*. Grenoble, Dec 1996, pp. 169–174.